Appendix A: Gelatin-Apatite Composites

This appendix contains an indentation variability study used to examine the mechanical behavior of biomimetic gelatin-apatite composite materials. The results are compared with similar studies on bone and dentin tissues contained in the main body of this work. A composite materials analysis of the gelatin-apatite materials is performed.

A.1 Biomimetic Composites for Modeling Bone

Much recent attention has been paid to tissue engineering and the formation of tissue-like materials *in vitro*. The extracellular matrix of mineralized tissues has been the focus of some of this attention, especially in the context of of generation of bone- and tooth-like materials from hydroxyapatite mineral formed *in vitro*.

A.1.1 Bone Tissue Engineering

Current clinical practice for bone replacement usually involves an autologous (from self) or allogenic (from a donor) bone transplant. Neither of these approaches is perfect—in autologous transplants, the bone may not be of sufficiently high quality, especially if there is a systemic condition affecting bone quality, and there exists the potential for donor site morbidity. In allogenic transplants, there exists a risk of disease transmission, especially viral, and immune responses to the foreign matter [Green et al, 2002]. This has led to substantial interest in creating artificial materials for use as bone substitutes in the body.

A number of approaches exist for bone tissue engineering or bone biomimetic material fabrication [Orban et al, 2002; Meyer et al, 2004a,b; Wiesmann et al, 2004]. Although many researchers have made bone-like composites by dispersing hydroxyapatite powders or granules in a polymeric matrix, the approach used to generate the materials studied here was a biomimetic co-precipitation process in which hydroxyapatite is formed *in situ* during the material fabrication. The following section contains a brief overview of the fabrication for this class of biomimetic materials.

A.1.2 Biomimetic Composite Fabrication

Biomimetic bone-like composite materials were generated by creating a

homogeneous suspension of $Ca(OH)_2$ and H_3PO_4 with gelatin [Chang et al, 2003a]. This suspension was gradually added to a reaction vessel through peristaltic pumps. The temperature of reaction solution in the vessel was maintained at 38°C and the pH was maintained at 8.0. The precipitated hydroxyapatite-gelatin slurry can then be dried at room temperature to form solid samples. The same general reaction procedure can be used to form nanocrystalline hydroxyapatite material when the reaction is carried out in the absence of gelatin. The composites can only be generated with relatively small weight fractions of gelatin, or the apatite crystal size decreases [Chang et al, 2003a]. The composites as thus formed are relatively uniform in nature, since gelatin lacks the ability of collagen to self-assemble to form long-range fibrillar structures. However, these materials provide an excellent organic-inorganic composite system to compare and contrast with bone, especially since the component gelatin and apatite phases can be examined independent of the composites.

A.2 Variability in Gelatin-Apatite Composites and Components

A.2.1 Components

Artificial bone-like nanocomposites can be constructed with phases of gelatin (denatured collagen) and apatite [Chang et al, 2003a]. In addition, pure gelatin and apatite samples may be made in the laboratory. This system provides a perfect opportunity for exploration of the mechanical response of biomineralized composite materials and their component phases directly.

First, to examine the component properties, nanoindentation experiments were performed under triangle-wave indentation conditions to different peak load levels at fixed rise time (as in section 3.3) on pure gelatin and on hydroxyapatite generated using the biomimetic process used for gelatin-apatite composites (section A.1.2 but with no gelatin added).

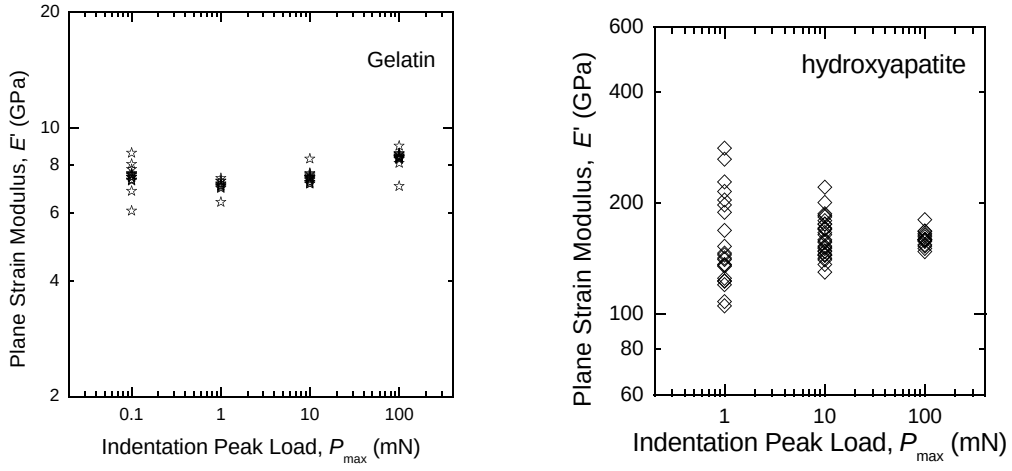

Figure A-1: (left) Variability in elastic modulus values for gelatin tested in an as-received condition. Responses are uniform and show little variability at any load. (right) Variability in elastic modulus values for polycrystalline apatite made in the laboratory There is some variability in the apatite indentation response at low loads.

Pure gelatin shows little variability on indentation testing (Figure A-1). Nanocrystalline hydroxyapatite shows scatter at small loads, but at large loads converges to an elastic modulus comparable to that of mineral (fluoro-)apatite (Figure 3-18).

A.2.2 Composites

Composite hydroxyapatite-gelatin materials with various gelatin contents were considered next. Raw load-displacement traces are presented in Figure A-2 for five individual 0.1 mN indentation tests on a nanocomposite material (gelatin-apatite composite "C"). In addition to there being variability in that the traces do not overlie, each individual traces demonstrates variability in changes of slope not consistent with the quadratic load-displacement response seen for homogeneous materials (see fused silica responses in Figure 3-16).

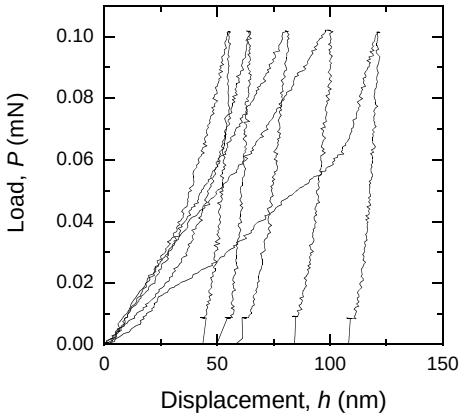

Figure A-2: Indentation load-displacement (*P*-*h*) responses for tests conducted at small load levels and in different locations on a gelatin-apatite composite material.

Representative data (individual data points for plane strain elastic modulus at each of four indentation peak loads) are shown in Figure A-3 for two nanocomposite materials (gelatin-apatite composites "I" and "C"). The diminishing variability with increasing

indentation peak load is evident in all nanocomposite gelatin-apatite materials, and at large (100 mN) indentation loads the modulus values converge to a narrow limit for all materials.

Two composites tested (A, J) showed an interesting variation on this trend. Instead of triangular wedge-shaped modulus-load (E'-P_{max}) plots with values converging to a single level but maintaining approximately comparable mean modulus at all load levels, composites A and J demonstrated a steep decrease in modulus with increasing indentation peak load. A representative plot of this alternative behavior is shown in Figure. A-4 for composite A. Although there is less variability in modulus at larger peak load levels, the overall response is dominated by a sharply decreasing trend in modulus with increasing indentation peak load and the convergence to a single-valued modulus at large load levels is less pronounced. The reasons for this behavior are unknown but porosity or other structural anomalies in the material are suspected.

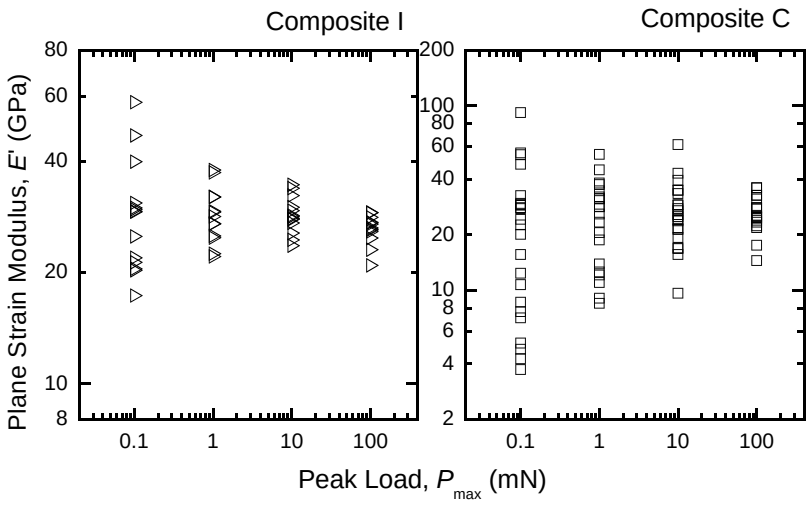

Figure A-3: Variability in elastic modulus values with indentation peak load level for two gelatin-apatite nanocomposites.

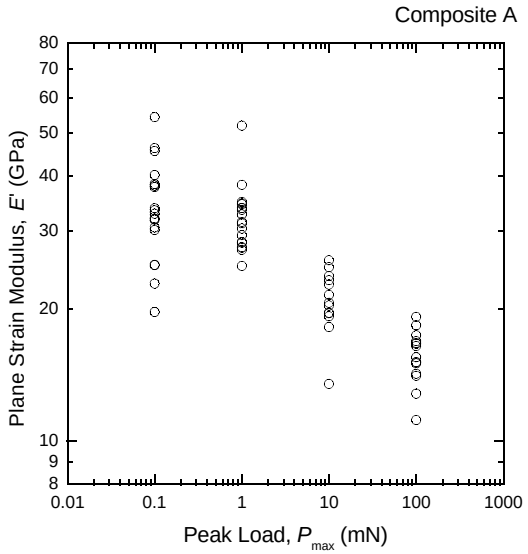

Figure A-4: Variability in elastic modulus values for a gelatin-apatite composite demonstrating a response dominated by decreasing modulus at increasing peak load level.

A.2.3 Materials Variability and Modulus Comparison

Mean (plane strain) elastic modulus values for hydroxyapatite and a number of gelatin-apatite composites are shown in Tables A-1 and A-2 for the tests performed at the smallest and largest experimental peak loads for each material. The fused silica control data from Chapter 3 (Tables 3-2 and 3-3) is replicated for comparison. Along with the mean plane strain modulus $(\bar{E}')$ for each data set, the standard deviations (*SD*) and coefficients of variation $(\%\,\mathrm{COV} = 100\,\%\,\bar{E}'/SD)$ are presented.

Table A-1: Small-depth (P_{max} = 0.1 or 1 mN) indentation variability for component and composite materials

	Peak Load level, Pmax	***Mean Plane Strain Modulus,*** $(\bar{E}')$	***Standard deviation (SD)***	***Percent Coefficient of Variation*** $100\,\%\,\bar{E}'/\mathrm{SD}$
Fused Silica	1 mN	69.39	4.64	6.7
Hydroxyapatite, polycrystalline	1 mN	164.03	50.36	30.7
Composite A	0.1 mN	34.37	8.37	24.3
Composite C	0.1 mN	24.89	21.25	85.4
Composite F	0.1 mN	23.14	11.23	48.6
Composite G	0.1 mN	29.52	6.11	20.7
Composite H	0.1 mN	29.95	7.86	26.3
Composite I	0.1 mN	29.96	11.33	37.8
Composite J	0.1 mN	34.88	6.4	18.3

Table A-2: Large-depth (P_{max} = 100 mN) indentation convergence for component and composite materials

	Mean $\bar{x}$ ***Plane Strain Modulus, E'***	***Standard deviation (SD)***	***Percent Coefficient of Variation*** $100\,\bar{x}/\mathrm{SD}$
Fused Silica	70.04	0.65	0.93
Hydroxyapatite	159.97	7.36	4.6
Composite A	15.72	2.03	12.9
Composite C	26.35	5.63	21.4
Composite F	24.49	2.42	9.9
Composite G	22.08	1.81	8.2
Composite H	25.25	2.3	9.1
Composite I	26.21	2.29	8.8
Composite J	19.05	0.78	4.1

At large depths, the indentation modulus data converge and the COV for the uniform materials and most composite materials drop to less than 10%. There are two artificial composites that do not obey this rule, maintaining more than 10% variability at 100 mN indentation loads, composites A and C, similar to the result seen in natural bone (Table 3-3). In the case of composite A, as was described earlier, the elastic modulus trend for this material was also different than the majority of the gelatin-apatite composites. In the case of Composite C, which was substantially more variable than any other composite over the entire range of indentation load levels and depths, there was a processing variation employed in the composite manufacture and this processing variation may have led to a substantial variation in apatite phase distribution compared to the other composite materials.

A.3 Composite Bounds and the Modulus of Gelatin-Apatite Composites

Importantly, the elastic modulus values of the gelatin-apatite composite materials are quite comparable to the mineralized tissues of bone and dentin. The values of plane strain modulus for the composites ranged from 16 to 26 GPa (E' at P_{max} = 100 mN) , intermediate to the modulus values of the gelatin (E' = 7.5 GPa at P_{max} = 10 mN) and hydroxyapatite (E' = 160 GPa at P_{max} = 100 mN) and comparable to the values for bone (E' = 19 GPa at P_{max} = 100 mN) and dentin (E' = 29 GPa at P_{max} = 100 mN).

The elastic modulus was calculated from plane strain modulus assuming $\nu = 0.3$ for the apatite and composites, and assuming $\nu = 0.49$ for gelatin. It was assumed that the elastic modulus at 100 mN was indicative of the continuum-level material responses for the composites. Volume fraction mineral was calculated from the weight fraction (Eqn 2-38) as if there was no porosity (Table A-3).

Table A-3: Gelatin-apatite component and composite elastic moduli and mineral composition

	E'	***E***	***Wf apatite***	***Vf apatite***
Gelatin	7.5	5.6	0	0
Hydroxyapatite	160	145	1	1
Composite A	15.72	14.31	0.94	0.83
Composite C	26.35	23.98	0.96	0.88
Composite F	24.49	22.29	0.90	0.74
Composite G	22.08	20.09	0.94	0.83
Composite H	25.25	22.98	0.94	0.83
Composite I	26.21	23.85	0.9	0.74
Composite J	19.05	17.34	0.85	0.64

The composite materials' modulus values can be compared with the predictions of the V-R and H-S bounds calculated from the gelatin and apatite values. The composites are shown along with the bounds in Figure A-8. Two conclusions are immediately

apparent: (1) there is no discernible trend for modulus with calculated volume fraction of mineral for the seven composites (A,C,F,G,H,I,J); (2) the modulus values seen in the composite materials fall closest to the lower bounds as graphed but are in many cases falling outside the modulus bounds. However, the composite modulus for these materials does not appear to be increasing much with increased mineral volume fraction. The obvious culprit for this is porosity: the weight fractions of mineral would be resulting in far lower mineral volume fractions in the composites than would be expected for a fully dense structure. With some estimate of the pore volume fraction, or a direct measurement of the mineral density in the composites, the volume fractions could be calculated and the modulus of the composites relative to the bounds could be re-evaluated. Further work will be required to examine the effects of porosity in these composite materials and to identify other factors that may play a role in determining the composite elastic modulus for these materials.

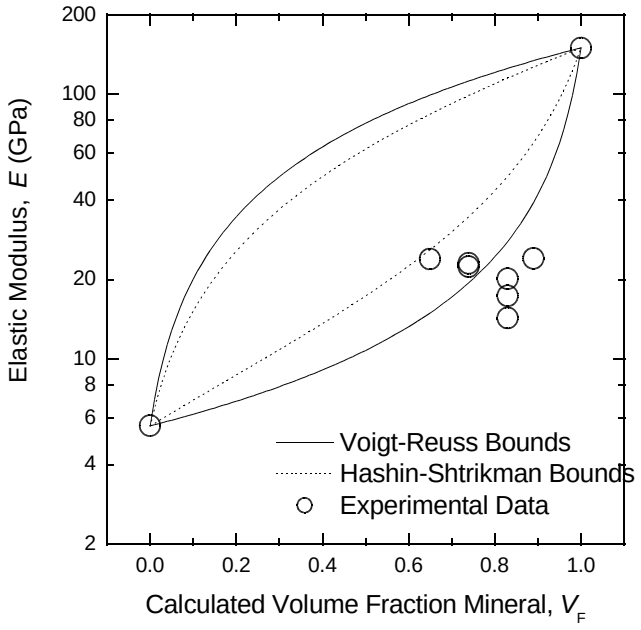

Figure A-5: Gelatin-apatite composites with calculated volume fractions (V_f) of mineral in the range 0.6 to 0.85 have modulus values (E) closest to the lower V-R or H-S modulus bounds based on the modulus values of the pure gelatin and apatite components.